tarjomehrooz.com 0902 795 28 76 ترجمه تخصصی توسط دکتری رشته مربوطه و برای کلیه زبان های خارجی + شبیه سازی مقالات با کلیه نرم افزار ها مثلب گمز و...

Unit Commitment Under Gas-Supply Uncertainty and Gas-Price Variability

Bining Zhao, *Student Member, IEEE,* Antonio J. Conejo, *Fellow, IEEE,* and Ramteen Sioshansi, *Senior Member, IEEE*

***Abstract*—We propose a two-stage mixed-integer linear stochastic optimization model to analyze the scheduling of electricity-production units under natural gas-supply uncertainty due to pipeline congestion and natural gas-price variability. The first stage of this stochastic optimization model represents the day-ahead scheduling (*i.e.*, unit commitment) stage, while the second stage represents actual real-time operations through a number of scenarios.**

We use this model to analyze the effect on unit commitment and dispatch of two types of natural gas-supply conditions. First, we analyze a case involving low-cost natural gas supply with natural gas-transmission issues related to potential natural gas-pipeline congestion. We then examine a case involving higher-cost natural gas, which is used solely to attain feasibility with fast-ramping events. The first case mimics situations in the ISO New England system, in which relatively low-cost natural gas supply is uncertain in cold-weather conditions due to natural gas-transmission bottlenecks. The second case is reminiscent of situations in the California ISO system, in which relatively expensive but flexible natural gas-fired units need to be used to handle rapid changes in net demand in the early mornings and late afternoons.

***Index Terms*—Unit commitment, natural gas supply, uncertainty, stochastic optimization.**

I. Introduction

THE amount of natural gas used as a primary energy source in power system operations has increased dramatically in recent years. Existing natural gas-fired generation accounted for about 42% of the total installed capacity in the United States in 2015 [1]. Given currently low natural gas prices, the electricity market is expected to introduce more natural gas-fired generation into power systems. Because many natural gas-fired units choose interruptible natural gas-supply contracts [2], the availability of natural gas supply can threaten the secure operation of electricity systems.

Several models are presented in the literature to study the impact of natural gas on power system operations. Munoz *et al*. [3] consider natural gas supply in power system-reliability studies. Quelhas *et al*. [4] study the economic interdependencies of electricity and various fuel-supply systems. Geidl *et al*. [5] present a model for optimization in coupling energy systems including electricity and natural gas systems. Liu *et al*. [6] present a security-constrained unit commitment model, which considers both natural gas pipeline-transportation and contracts limits. Li *et al*. [7] consider units that can switch generating fuels in a security-constrained unit commitment. They incorporate a set of natural gas constraints based on daily and hourly natural gas-pipeline capacity. Both Qadrdan *et al*. [8] and Alabdulwahab *et al*. [9] present studies of firming wind power in an integrated natural gas and electricity network. Qadrdan *et al*. [8] provide a set of nonlinear natural gas transportation constraints that consider natural gas flow, compressors, and linepack within the natural gas-pipeline network. Alabdulwahab *et al*. [9] model both natural gas contract limits and transportation constraints. Liu *et al*. [10] present a linearly approximated natural gas flow model embedded within a robust unit commitment model. Alabdulwahab *et al*. [2] introduce a stochastic security-constrained unit commitment model that integrates natural gas pipeline-transportation constraints.

In this paper, we propose a two-stage stochastic unit commitment model that integrates natural gas-supply constraints into the commitment and dispatch processes. As is customary in stochastic optimization models, this uncertainty is modeled via scenarios. For sake of simplicity and to focus on the effect of natural gas-supply shortages (as a result of natural gas-pipeline issues) on the electrical system, we do not include a detailed representation of the natural gas-pipeline system. However, such detailed representation can be easily incorporated into the proposed model.

Our model follows formative works on mixed-integer linear unit commitment [11] and two-stage stochastic electricity market-clearing models [12]. We formulate this problem as having day-ahead unit commitment decisions in the first stage, with real-time dispatch and market-balancing decisions in the second stage. The proposed model assumes a set of known real-time demands, and can thus be used for day-ahead market-clearing. As such, the model is prognostic of real-time operations, based on forecasted demand, in the stochastic optimization sense. The objective of the model is to minimize the sum of day-ahead commitment and expected real-time dispatch costs. We consider both hourly and daily natural gas-supply constraints. The former are intended to represent physical constraints on instantaneous pipeline flows while the latter represent a limit on the amount of fuel that is contracted for delivery during the day. The scenarios in the stochastic optimization model capture uncertainties in the hourly natural

This work was supported by NSF grants 1548015, 1423316, 1442686, 1508993, and 1509040.

B. Zhao is with the Electrical and Computer Engineering Department, The Ohio State University, Columbus, OH 43210, USA (e-mail: zhao.1418@osu.edu).

A. J. Conejo is with the Integrated Systems Engineering and Electrical and Computer Engineering Departments, The Ohio State University, Columbus, OH 43210, USA (e-mail: conejonavarro.1@osu.edu).

R. Sioshansi is with the Integrated Systems Engineering Department, The Ohio State University, Columbus, OH 43210, USA (e-mail: sioshansi.1@osu.edu).

tarjomehrooz.com 0902 795 28 76 ترجمه تخصصی توسط دکتری رشته مربوطه و برای کلیه زبان های خارجی + شبیه سازی مقالات با کلیه نرم افزار ها مثلب گمز و ...

gas-pipeline capacities. These scenarios, which are inputs to the model, can easily represent any physical condition of the natural gas-supply system (*e.g.*, reduced or no pipeline capacity). The extent to which natural gas-supply scenarios have major impacts on electricity system operations depends on how much the generation mix relies on natural gas-fired units. To clearly show the effect on electricity system operations of natural gas-supply shortages (which is the focus of this paper), we neglect uncertainties other that those pertaining to natural gas supply. Incorporating other sources of uncertainty can be easily done. The proposed model can also be refined by employing reserve policies that depend on the extent of the uncertainty [13], [14].

We use our proposed model to study the effects of natural gas-supply constraints on power system operations under two system paradigms that are becoming increasingly common today. The first is a case in which natural gas prices are relatively low but potential natural gas-pipeline congestion limits the extent to which the system can rely on natural gas-fired units. The second case has relatively high natural gas prices, but the flexibility of natural gas-fired units must be used to accommodate steep ramps in the load profile. The first case is reminiscent of the ISO New England system [1], where few natural gas-fired units hold firm fuel-supply contracts. Thus, the system faces potential natural gas-supply constraints during cold winter days [1]. The second case is based on the California ISO system [15], which is facing fast-ramping conditions due to diurnal wind and solar production patterns. We examine the effects of these two types of natural gas supply conditions on unit commitment, dispatch, and day-ahead energy prices.

This work and our choice of the two system paradigms examined are motivated by recent events in the ISO New England [1] and California ISO [16] systems. The overarching goal of the work is to reveal insights into the effects of having power systems with increasing penetrations of natural gas-fired generation, which we believe to be of value to the power system engineering community. This paper makes two contributions, which add to the existing literature studying the interactions of electricity- and natural gas-supply networks:

1) developing a stochastic unit commitment model with a representation of the constraints imposed by the natural gas-supply network, and
2) carrying out detailed numeral simulations involving (a) stochastic natural gas-supply uncertainty and (b) -price variability.

The remainder of this paper is organized as follows. The formulation of the proposed model is detailed in Section II. Section III presents and analyzes a simple example based on a four-node transmission network under the two natural gas-supply paradigms discussed above. Section IV conducts the same analysis using an eight-zone test system based on the ISO New England system [17] and a 240-node system based on the Western Electricity Coordinating Council (WECC) area [18]. Section V concludes.

II. Model Formulation

This section provides a detailed formulation of the proposed model. We first introduce the model notation followed by the mathematical formulation of the model.

A. Notation

Sets and Indices

Δ	Set of natural gas pipelines
Δ_p	Set of natural gas-fired units connected to pipeline p
Λ	Set of buses
Λ_n	Set of buses directly connected to bus n by a transmission line
Ξ	Set of scenarios
Ω^{G}	Set of natural gas-fired units
Ω^{G}_n	Set of natural gas-fired units connected to bus n
Ω^{T}	Set of thermal units
Ω^{T}_n	Set of thermal units connected to bus n
g	Index of natural gas-fired units
i	Index of thermal units

Constants

m, n	Index of system buses
p	Index of natural gas pipelines
t	Index of time periods
ξ	Index of scenarios
REF	Reference bus with phase angle fixed equal to 0
b_g	Heat rate of natural gas-fired unit g [MBTU/MWh]
$B_{n,m}$	Susceptance of transmission line connecting buses n and m [p.u.]
c^{G}_g	Marginal cost of natural gas-fired unit g [$/MWh]
c^{T}_i	Marginal cost of thermal unit i [$/MWh]
$C^{\mathrm{G,NL}}_g$	No-load cost of natural gas-fired unit g [$]
$C^{\mathrm{G,SU}}_g$	Start-up cost of natural gas-fired unit g [$]
$C^{\mathrm{T,NL}}_i$	No-load cost of thermal unit i [$]
$C^{\mathrm{T,SU}}_i$	Start-up cost of thermal unit i [$]
$C^{\max}_{n,m}$	Capacity of transmission line connecting buses n and m [MW]
$F^{\mathrm{G,NL}}_g$	No-load gas consumption of natural gas-fired unit g [MBTU]
$F^{\mathrm{G,SU}}_g$	Start-up gas consumption of natural gas-fired unit g [MBTU]
$F^{\max}_{p,\xi,t}$	Hour-t capacity of natural-gas pipeline p in scenario ξ [MBTU]
$F^{\max}_p$	One-day contract limit of natural-gas pipeline p [MBTU]
$L_{n,t}$	Hour-t load at bus n [MW]
$P^{\mathrm{G,max}}_g$	Generating capacity of natural gas-fired unit g [MW]
$P^{\mathrm{G,min}}_g$	Minimum-generation level of natural gas-fired unit g [MW]
$P^{\mathrm{T,max}}_i$	Generating capacity of thermal unit i [MW]
$P^{\mathrm{T,min}}_i$	Minimum-generation level of thermal unit i [MW]
$R^{\mathrm{G,D}}_g$	Maximum downward reserve of natural gas-fired unit g [MW]
$R^{\mathrm{G,U}}_g$	Maximum upward reserve of natural gas-fired unit g [MW]

tarjomehrooz.com 0902 795 28 76 ترجمه تخصصی توسط دکتری رشته مربوطه و برای کلیه زبان های خارجی + شبیه سازی مقالات با کلیه نرم افزار ها مثل گمز و ...

$R_i^{\mathrm{T,D}}$ Maximum downward reserve of thermal unit i [MW]
$R_i^{\mathrm{T,U}}$ Maximum upward reserve of thermal unit i [MW]
RD_g^{G} Downward ramping limit of natural gas-fired unit g [MW/hour]
RD_i^{T} Downward ramping limit of thermal unit i [MW/hour]
RU_g^{G} Upward ramping limit of natural gas-fired unit g [MW/hour]
RU_i^{T} Upward ramping limit of thermal unit i [MW/hour]
T Number of hours in the study horizon
V^{LOL} Value of lost of load [$/MWh]
π_ξ Probability of scenario ξ
ρ Natural gas price [$/MBTU]

Variables

$F_{g,t}^{\mathrm{G}}$ Hour-t natural gas consumption of natural gas-fired unit g in the scheduling stage [MBTU]
$F_{p,t}^{\mathrm{S}}$ Hour-t natural gas flow through pipeline p in the scheduling stage [MBTU]
$f_{g,\xi,t}^{\mathrm{G}}$ Hour-t change in natural gas consumption of natural gas-fired unit g in scenario-ξ operating stage [MBTU]
$L_{n,\xi,t}^{\mathrm{SHED}}$ Hour-t load shed at node n in scenario ξ operating stage [MW]
$P_{g,t}^{\mathrm{G}}$ Hour-t production of natural gas-fired unit g in the scheduling stage [MW]
$P_{i,t}^{\mathrm{T}}$ Hour-t production of thermal unit i in the scheduling stage [MW]
$r_{g,\xi,t}^{\mathrm{G,D}}$ Hour-t downward reserve of natural gas-fired unit g deployed in scenario ξ operating stage [MW]
$r_{g,\xi,t}^{\mathrm{G,U}}$ Hour-t upward reserve of natural gas-fired unit g deployed in scenario ξ operating stage [MW]
$r_{i,\xi,t}^{\mathrm{T,D}}$ Hour-t downward reserve of thermal unit i deployed in scenario ξ operating stage [MW]
$r_{i,\xi,t}^{\mathrm{T,U}}$ Hour-t upward reserve of thermal unit i deployed in scenario ξ operating stage [MW]
$x_{g,t}^{\mathrm{G}}$ Hour-t commitment status of natural gas-fired unit g: equals 1 if on, 0 otherwise
$x_{i,t}^{\mathrm{T}}$ Hour-t commitment status of thermal unit i: equals 1 if on, 0 otherwise
$y_{g,t}^{\mathrm{G}}$ Hour-t startup indicator of natural gas-fired unit g: equals 1 if started up at the beginning of hour t, 0 otherwise
$y_{i,t}^{\mathrm{T}}$ Hour-t startup indicator of thermal unit i: equals 1 if started up at the beginning of hour t, 0 otherwise
$z_{g,t}^{\mathrm{G}}$ Hour-t shutdown indicator of natural gas-fired unit g: equals 1 if shutdown at the beginning of hour t, 0 otherwise
$z_{i,t}^{\mathrm{T}}$ Hour-t shutdown indicator of thermal unit i: equals 1 if shutdown at the beginning of hour t, 0 otherwise
$\theta_{n,t}^{0}$ Hour-t phase angle of node n in the the scheduling stage [rad]
$\theta_{n,\xi,t}$ Hour-t phase angle of node n in scenario ξ operating stage [rad]

B. Optimization Model

We now detail the formulation of the optimization model, which has two types of constraints. The first, which consists of constraint sets (2)–(11), represents the scheduling stage, when day-ahead unit commitment decisions are made. The second, consisting of constraint sets (12)–(28), represent the operating stage, when per-scenario real-time operations are determined.

$$\min \sum_{t=1}^{T} \Bigg\{ \sum_{i\in\Omega^{\mathrm{T}}} \left(y_{i,t}^{\mathrm{T}} C_i^{\mathrm{T,SU}} + x_{i,t}^{\mathrm{T}} C_i^{\mathrm{T,NL}} + c_i^{\mathrm{T}} P_{i,t}^{\mathrm{T}} \right) + \sum_{g\in\Omega^{\mathrm{G}}} \left(\rho F_{g,t}^{\mathrm{G}} + y_{g,t}^{\mathrm{G}} C_g^{\mathrm{G,SU}} + x_{g,t}^{\mathrm{G}} C_g^{\mathrm{G,NL}} + c_g^{\mathrm{G}} P_{g,t}^{\mathrm{G}} \right) + \sum_{\xi\in\Xi} \pi_\xi \cdot \Bigg(\sum_{i\in\Omega^{\mathrm{T}}} c_i^{\mathrm{T}} \cdot \left(r_{i,\xi,t}^{\mathrm{T,U}} - r_{i,\xi,t}^{\mathrm{T,D}} \right) + \sum_{g\in\Omega^{\mathrm{G}}} \rho f_{g,\xi,t}^{\mathrm{G}} + \sum_{g\in\Omega^{\mathrm{G}}} c_g^{\mathrm{G}} \cdot \left(r_{g,\xi,t}^{\mathrm{G,U}} - r_{g,\xi,t}^{\mathrm{G,D}} \right) + \sum_{n\in\Lambda} V^{\mathrm{LOL}} L_{n,\xi,t}^{\mathrm{SHED}} \Bigg) \Bigg\} \quad (1)$$

$$\text{s.t.} \sum_{i\in\Omega_n^{\mathrm{T}}} P_{i,t}^{\mathrm{T}} + \sum_{g\in\Omega_n^{\mathrm{G}}} P_{g,t}^{\mathrm{G}} - L_{n,t} = \sum_{m\in\Lambda_n} B_{n,m} \cdot (\theta_{n,t}^0 - \theta_{m,t}^0); \forall n \in \Lambda, t \in T; \quad (2)$$

$$\theta_{\mathrm{REF},t}^0 = 0; \forall t \in T; \quad (3)$$

$$x_{g,t}^{\mathrm{G}} P_g^{\mathrm{G,min}} \le P_{g,t}^{\mathrm{G}} \le x_{g,t}^{\mathrm{G}} P_g^{\mathrm{G,max}}; \forall g \in \Omega^{\mathrm{G}}, t \in T; \quad (4)$$

$$x_{i,t}^{\mathrm{T}} P_i^{\mathrm{T,min}} \le P_{i,t}^{\mathrm{T}} \le x_{i,t}^{\mathrm{T}} P_i^{\mathrm{T,max}}; \forall i \in \Omega^{\mathrm{T}}, t \in T; \quad (5)$$

$$F_{g,t}^{\mathrm{G}} = b_g P_{g,t}^{\mathrm{G}} + F_g^{\mathrm{G,NL}} x_{g,t}^{\mathrm{G}} + F_g^{\mathrm{G,SU}} y_{g,t}^{\mathrm{G}}; \forall g \in \Omega^{\mathrm{G}}, t \in T; \quad (6)$$

$$F_{p,t}^{\mathrm{S}} = \sum_{g\in\Delta_p} F_{g,t}^{\mathrm{G}}; \forall p \in \Delta, t \in T; \quad (7)$$

$$y_{g,t}^{\mathrm{G}} - z_{g,t}^{\mathrm{G}} = x_{g,t}^{\mathrm{G}} - x_{g,t-1}^{\mathrm{G}}; \forall g \in \Omega^{\mathrm{G}}, t \in T; \quad (8)$$

$$y_{i,t}^{\mathrm{T}} - z_{i,t}^{\mathrm{T}} = x_{i,t}^{\mathrm{T}} - x_{i,t-1}^{\mathrm{T}}; i \in \Omega^{\mathrm{T}}, \forall t \in T; \quad (9)$$

$$x_{g,t}^{\mathrm{G}}, y_{g,t}^{\mathrm{G}}, z_{g,t}^{\mathrm{G}} \in \{0,1\}; \forall g \in \Omega^{\mathrm{G}}, t \in T; \quad (10)$$

$$x_{i,t}^{\mathrm{T}}, y_{i,t}^{\mathrm{T}}, z_{i,t}^{\mathrm{T}} \in \{0,1\}; \forall i \in \Omega^{\mathrm{T}}, t \in T; \quad (11)$$

$$\sum_{i\in\Omega_n^{\mathrm{T}}} (r_{i,\xi,t}^{\mathrm{T,U}} - r_{i,\xi,t}^{\mathrm{T,D}}) + \sum_{g\in\Omega_n^{\mathrm{G}}} (r_{g,\xi,t}^{\mathrm{G,U}} - r_{g,\xi,t}^{\mathrm{G,D}}) + L_{n,\xi,t}^{\mathrm{SHED}} = \sum_{m\in\Lambda_n} B_{n,m} \cdot (\theta_{n,t}^0 - \theta_{n,\xi,t} - \theta_{m,t}^0 + \theta_{m,\xi,t}); \quad (12)$$

$$\forall n \in \Lambda, t \in T, \xi \in \Xi;$$

$$\theta_{\mathrm{REF},\xi,t} = 0; \forall t \in T, \xi \in \Xi; \quad (13)$$

$$-C_{n,m}^{\max} \le B_{n,m} \cdot (\theta_{n,\xi,t} - \theta_{m,\xi,t}) \le C_{n,m}^{\max}; \quad (14)$$

$$\forall n \in \Lambda, m \in \Lambda_n, t \in T, \xi \in \Xi;$$

$$0 \le L_{n,\xi,t}^{\mathrm{SHED}} \le L_{n,t}; \forall n \in \Lambda, t \in T, \xi \in \Xi; \quad (15)$$

$$x_{g,t}^{\mathrm{G}} P_g^{\mathrm{G,min}} \le P_{g,t}^{\mathrm{G}} + (r_{g,\xi,t}^{\mathrm{G,U}} - r_{g,\xi,t}^{\mathrm{G,D}}) \le x_{g,t}^{\mathrm{G}} P_g^{\mathrm{G,max}}; \forall g \in \Omega^{\mathrm{G}}, t \in T, \xi \in \Xi; \quad (16)$$

$$0 \le r_{g,\xi,t}^{\mathrm{G,U}} \le x_{g,t}^{\mathrm{G}} R_g^{\mathrm{G,U}}; \forall g \in \Omega^{\mathrm{G}}, t \in T, \xi \in \Xi; \quad (17)$$

$$0 \le r_{g,\xi,t}^{\mathrm{G,D}} \le x_{g,t}^{\mathrm{G}} R_g^{\mathrm{G,D}}; \forall g \in \Omega^{\mathrm{G}}, t \in T, \xi \in \Xi; \quad (18)$$

$$(P_{g,t}^{\mathrm{G}} + r_{g,\xi,t}^{\mathrm{G,U}} - r_{g,\xi,t}^{\mathrm{G,D}}) - (P_{g,t-1}^{\mathrm{G}} + r_{g,\xi,t-1}^{\mathrm{G,U}} - r_{g,\xi,t-1}^{\mathrm{G,D}}) \le RU_g^{\mathrm{G}}; \forall g \in \Omega^{\mathrm{G}}, t \in T, \xi \in \Xi; \quad (19)$$

tarjomehrooz.com 0902 795 28 76 ترجمه تخصصی توسط دکتری رشته مربوطه و برای کلیه زبان های خارجی + شبیه سازی مقالات با کلیه نرم افزار ها مثلب گمز و ...

$$(P^{\mathrm{G}}_{g,t-1} + r^{\mathrm{G,U}}_{j,\xi,t-1} - r^{\mathrm{G,D}}_{g,\xi,t-1}) - (P^{\mathrm{G}}_{g,t} + r^{\mathrm{G,U}}_{g,\xi,t} - r^{\mathrm{G,D}}_{g,\xi,t}) \leq RD^{\mathrm{G}}_{g}; \forall g \in \Omega^{\mathrm{G}}, t \in T, \xi \in \Xi; \quad (20)$$

$$x^{\mathrm{T}}_{i,t} P^{\mathrm{T,min}}_{i} \leq P^{\mathrm{T}}_{i,t} + (r^{\mathrm{T,U}}_{i,\xi,t} - r^{\mathrm{T,D}}_{i,\xi,t}) \leq x^{\mathrm{T}}_{i,t} P^{\mathrm{T,max}}_{i}; \quad (21)$$
$$\forall i \in \Omega^{\mathrm{T}}, t \in T, \xi \in \Xi;$$

$$0 \leq r^{\mathrm{T,U}}_{i,\xi,t} \leq x^{\mathrm{T}}_{i,t} R^{\mathrm{T,U}}_{i}; \forall i \in \Omega^{\mathrm{T}}, t \in T, \xi \in \Xi; \quad (22)$$

$$0 \leq r^{\mathrm{T,D}}_{i,\xi,t} \leq x^{\mathrm{T}}_{i,t} R^{\mathrm{T,D}}_{i}; \forall i \in \Omega^{\mathrm{T}}, t \in T, \xi \in \Xi; \quad (23)$$

$$(P^{\mathrm{T}}_{i,t} + r^{\mathrm{T,U}}_{i,\xi,t} - r^{\mathrm{T,D}}_{i,\xi,t}) - (P^{\mathrm{T}}_{i,t-1} + r^{\mathrm{T,U}}_{i,\xi,t-1} - r^{\mathrm{T,D}}_{i,\xi,t-1}) \leq RU^{\mathrm{T}}_{i}; \forall i \in \Omega^{\mathrm{T}}, t \in T, \xi \in \Xi; \quad (24)$$

$$(P^{\mathrm{T}}_{i,t-1} + r^{\mathrm{T,U}}_{i,\xi,t-1} - r^{\mathrm{T,D}}_{i,\xi,t-1}) - (P^{\mathrm{T}}_{i,t} + r^{\mathrm{T,U}}_{i,\xi,t} - r^{\mathrm{T,D}}_{i,\xi,t}) \leq RD^{\mathrm{T}}_{i}; \forall i \in \Omega^{\mathrm{T}}, t \in T, \xi \in \Xi; \quad (25)$$

$$f^{\mathrm{G}}_{g,\xi,t} = b_g \cdot (r^{\mathrm{G,U}}_{g,\xi,t} - r^{\mathrm{G,D}}_{g,\xi,t}); \quad (26)$$
$$\forall g \in \Omega^{\mathrm{G}}, t \in T, \xi \in \Xi;$$

$$F^{\mathrm{S}}_{p,t} + \sum_{g \in \Delta_p} f^{\mathrm{G}}_{g,\xi,t} \leq F^{\max}_{p,\xi,t}; \forall p \in \Delta, t \in T, \xi \in \Xi; \quad (27)$$

$$\sum_{t=1}^{T} (F^{\mathrm{S}}_{p,t} + \sum_{g \in \Delta_p} f^{\mathrm{G}}_{g,\xi,t}) \leq F^{\max}_{p}; \forall p \in \Delta, \xi \in \Xi. \quad (28)$$

Objective function (1) minimizes the total expected operational costs of all thermal and natural gas-fired units over the T-hour model horizon. This objective consists of several terms. The first two terms represent the cost of committing and scheduling thermal and natural gas-fired units in the day-ahead scheduling stage.

For reasons of generality, we assume that natural gas-fired plants incur two types of costs. The first is a fuel cost, which depends on the amount of natural gas consumed for generator startups, no-load fuel use, and actual electricity production. The second are non-fuel costs, which are also associated with generator startups, no-load, and actual production. These latter costs can encompass variable operations and maintenance, among other costs. Fuel cost is computed by calculating the total amount of natural gas consumed by a natural gas-fired unit and multiplying this quantity by the assumed natural gas price.

The remaining objective-function terms represent the expected cost of operating the thermal and natural gas-fired units and the system in real-time. Specifically, the:

$$\sum_{i \in \Omega^{\mathrm{T}}} c^{\mathrm{T}}_{i} \cdot \left(r^{\mathrm{T,U}}_{i,\xi,t} - r^{\mathrm{T,D}}_{i,\xi,t} \right),$$

term represents the cost of adjusting the output of thermal generators in real-time, the:

$$\sum_{g \in \Omega^{\mathrm{G}}} \left[\rho f^{\mathrm{G}}_{g,\xi,t} + c^{\mathrm{G}}_{g} \cdot \left(r^{\mathrm{G,U}}_{g,\xi,t} - r^{\mathrm{G,D}}_{g,\xi,t} \right) \right],$$

term represents the cost of adjusting the output of natural gas-fired generators in real-time (including incremental natural gas costs), and the:

$$\sum_{n \in \Lambda} V^{\mathrm{LOL}} L^{\mathrm{SHED}}_{n,\xi,t},$$

term represents the cost of any load that must be shed in real-time.

As noted before, the proposed model has two types of constraints. The first, consisting of constraint sets (2)–(11), impose day-ahead scheduling-stage restrictions. Constraints (2) enforce load-balance at each node in the scheduling stage. The left-hand side of each equality is the total power generated by all of the units connected to bus n in hour t, less the load at that node. The right-hand side of the equality gives the total net power flow in hour t through the transmission lines directly connected to node n. We assume a well designed power system that is able to supply the demand under normal operating conditions. Thus, load shedding is not considered at the scheduling stage, which represents an average normal condition. Load shedding is, however, considered at the operating stage in the event of an extreme natural gas-supply scenario. Load-balance is imposed at the scheduling stage in the model to be able to compute day-ahead locational marginal prices (LMPs), once binary variables are fixed to their optimal values. In this way we can examine the impacts of natural gas-supply conditions on day-ahead LMPs. Because LMPs are computed using dual variables of equality constraints, they can be negative.

Constraints (3) fix the phase angle at the reference node to zero in each hour at the scheduling stage. Constraints (4) and (5) impose minimum- and maximum-generating capacities on the natural gas-fired and thermal units, respectively. Constraints (6) and (7) define fuel usage of each natural gas-fired unit and total pipeline capacity scheduled for use in each hour at the scheduling stage.

Constraints (8) and (9) impose the state transitions that define the values of the y and z variables for the natural gas-fired and thermal units, respectively, in terms of changes in the x variables from one hour to the next. Constraints (10) and (11) require these variables to take on binary values.

The remaining constraints impose operating-stage restrictions. Constraints (12) impose hourly nodal load-balance. We define real-time load-balance in terms of incremental changes (relative to the scheduling stage) in generation and load shed on the left-hand sides of the equalities. The right-hand sides of the equalities give incremental changes in power flows, which are based on incremental changes (relative to the scheduling stage) in phase angles. The operating-stage load-balance constraints are formulated in this manner (*i.e.*, in terms of incremental changes relative to the scheduling stage) to avoid redundancy with the scheduling-stage load-balance constraints. If such redundancy is included in the constraints, dual variables cannot be reliably used to compute LMPs.

Constraints (13) fix the phase angles at the reference node to zero. Constraints (14) impose the flow limits on each transmission line in each scenario and hour. The flow limits are represented at the operating stage, which is when they are relevant in the sense that they may be binding. Thus, these constraints do not need to be represented at the scheduling stage. Constraints (15) restrict load shedding to be less than actual load in each hour.

Constraints (16)–(20) are technical limits on the operations of natural gas-fired units. Constraints (16) impose minimum and maximum generating capacities on natural gas-fired units. Constraints (17) and (18) enforce upward and downward reserve limits, respectively, for natural gas-fired

tarjomehrooz.com 0902 795 28 76 ترجمه تخصصی توسط دکتری رشته مربوطه و برای کلیه زبان های خارجی + شبیه سازی مقالات با کلیه نرم افزار ها مثلب گمز و ...

units. Constraints (19) and (20) impose upward and downward ramping restrictions on natural gas-fired units, respectively. Constraints (21)–(25) are analogous technical restrictions on the operation of thermal units. Because ramping limits are represented at the operating stage, which is when they are relevant in the sense that they may be binding, they do not need to be represented at the scheduling stage.

Finally, constraints (26) compute incremental (relative to the scheduling stage) fuel usage by each natural gas-fired unit in each hour of each scenario. Constraints (27) and (28) impose the two types of natural gas-supply constraints discussed in the introduction. Specifically, constraints (27) are physical pipeline-capacity restrictions in each hour while constraints (28) impose the contract limit on daily natural gas use.

C. Value of Stochastic Solution Computations

One way that we demonstrate the benefits of our proposed two-stage stochastic planning model is by computing the value of stochastic solution (VSS). VSS gives an estimate of the benefit of modeling uncertainty when making stage-1 unit commitment decisions [19].

We compute the VSS by first solving the following deterministic version of the model introduced in Section II-B in which the uncertain natural gas-pipeline capacities, $F^{\max}_{p,\xi,t}$, are replaced by their expected values:

$$\bar{F}^{\max}_{p,t} = \sum_{\xi \in \Xi} \pi_\xi F^{\max}_{p,\xi,t}.$$

This model is formulated as:

$$\min \sum_{t=1}^{T} \left\{ \sum_{i \in \Omega^{\mathrm{T}}} \left(y^{\mathrm{T}}_{i,t} C^{\mathrm{T,SU}}_i + x^{\mathrm{T}}_{i,t} C^{\mathrm{T,NL}}_i + c^{\mathrm{T}}_i P^{\mathrm{T}}_{i,t} \right) \right. \tag{29}$$
$$\left. + \sum_{g \in \Omega^{\mathrm{G}}} \left(\rho F^{\mathrm{G}}_{g,t} + y^{\mathrm{G}}_{g,t} C^{\mathrm{G,SU}}_g + x^{\mathrm{G}}_{g,t} C^{\mathrm{G,NL}}_g + c^{\mathrm{G}}_g P^{\mathrm{G}}_{g,t} \right) \right\}$$

$$\text{s.t.} \sum_{i \in \Omega^{\mathrm{T}}_n} P^{\mathrm{T}}_{i,t} + \sum_{g \in \Omega^{\mathrm{G}}_n} P^{\mathrm{G}}_{g,t} - L_{n,t} \tag{30}$$
$$= \sum_{m \in \Lambda_n} B_{n,m} \cdot (\theta^0_{n,t} - \theta^0_{m,t}); \forall n \in \Lambda, t \in T;$$

$$\theta^0_{\mathrm{REF},t} = 0; \forall t \in T; \tag{31}$$

$$x^{\mathrm{G}}_{g,t} P^{\mathrm{G,min}}_g \le P^{\mathrm{G}}_{g,t} \le x^{\mathrm{G}}_{g,t} P^{\mathrm{G,max}}_g; \forall g \in \Omega^{\mathrm{G}}, t \in T; \tag{32}$$

$$x^{\mathrm{T}}_{i,t} P^{\mathrm{T,min}}_i \le P^{\mathrm{T}}_{i,t} \le x^{\mathrm{T}}_{i,t} P^{\mathrm{T,max}}_i; \forall i \in \Omega^{\mathrm{T}}, t \in T; \tag{33}$$

$$F^{\mathrm{G}}_{g,t} = b_g P^{\mathrm{G}}_{g,t} + F^{\mathrm{G,NL}}_g x^{\mathrm{G}}_{g,t} + F^{\mathrm{G,SU}}_g y^{\mathrm{G}}_{g,t}; \tag{34}$$
$$\forall g \in \Omega^{\mathrm{G}}, t \in T;$$

$$F^{\mathrm{S}}_{p,t} = \sum_{g \in \Delta_p} F^{\mathrm{G}}_{g,t}; \forall p \in \Delta, t \in T; \tag{35}$$

$$y^{\mathrm{G}}_{g,t} - z^{\mathrm{G}}_{g,t} = x^{\mathrm{G}}_{g,t} - x^{\mathrm{G}}_{g,t-1}; \forall g \in \Omega^{\mathrm{G}}, t \in T; \tag{36}$$

$$y^{\mathrm{T}}_{i,t} - z^{\mathrm{T}}_{i,t} = x^{\mathrm{T}}_{i,t} - x^{\mathrm{T}}_{i,t-1}; i \in \Omega^{\mathrm{T}}, \forall t \in T; \tag{37}$$

$$x^{\mathrm{G}}_{g,t}, y^{\mathrm{G}}_{g,t}, z^{\mathrm{G}}_{g,t} \in \{0,1\}; \forall g \in \Omega^{\mathrm{G}}, t \in T; \tag{38}$$

$$x^{\mathrm{T}}_{i,t}, y^{\mathrm{T}}_{i,t}, z^{\mathrm{T}}_{i,t} \in \{0,1\}; \forall i \in \Omega^{\mathrm{T}}, t \in T; \tag{39}$$

$$-C^{\max}_{n,m} \le B_{n,m} \cdot (\theta_{n,t} - \theta_{m,t}) \le C^{\max}_{n,m}; \tag{40}$$
$$\forall n \in \Lambda, m \in \Lambda_n, t \in T;$$

$$P^{\mathrm{G}}_{g,t} - P^{\mathrm{G}}_{g,t-1} \le RU^{\mathrm{G}}_g; \forall g \in \Omega^{\mathrm{G}}, t \in T; \tag{41}$$

$$P^{\mathrm{G}}_{g,t-1} - P^{\mathrm{G}}_{g,t} \le RD^{\mathrm{G}}_g; \forall g \in \Omega^{\mathrm{G}}, t \in T; \tag{42}$$

$$P^{\mathrm{T}}_{i,t} - P^{\mathrm{T}}_{i,t-1} \le RU^{\mathrm{T}}_i; \forall i \in \Omega^{\mathrm{T}}, t \in T; \tag{43}$$

$$P^{\mathrm{T}}_{i,t-1} - P^{\mathrm{T}}_{i,t} \le RD^{\mathrm{T}}_i; \forall i \in \Omega^{\mathrm{T}}, t \in T; \tag{44}$$

$$F^{\mathrm{S}}_{p,t} \le \bar{F}^{\max}_{p,t}; \forall p \in \Delta, t \in T; \tag{45}$$

$$\sum_{t=1}^{T} F^{\mathrm{S}}_{p,t} \le F^{\max}_p; \forall p \in \Delta. \tag{46}$$

Objective function (29) is the same as that of the stochastic problem, except that there are no recourse decisions and, as such, no second-stage cost. Constraints (30)–(39) are identical to constraints (2)–(11) of the stochastic model. Constraints (40)–(46) impose operating-stage constraints from the stochastic model on the deterministic problem. Specifically, constraints (40) impose flow limits on transmission lines, constraints (41)–(44) impose ramping limits and constraints (45) and (46) impose natural gas capacities. Constraints (45) are analogous to constraints (27), except that natural gas usage is restricted to the expected capacity of each pipeline in each hour.

Once this deterministic problem is solved, the values of the scheduling-stage variables (*i.e.*, $F^{\mathrm{G}}_{g,t}$, $F^{\mathrm{S}}_{p,t}$, $P^{\mathrm{G}}_{g,t}$, $P^{\mathrm{T}}_{i,t}$, $x^{\mathrm{G}}_{g,t}$, $x^{\mathrm{T}}_{i,t}$, $y^{\mathrm{G}}_{g,t}$, $y^{\mathrm{T}}_{i,t}$, $z^{\mathrm{G}}_{g,t}$, $z^{\mathrm{T}}_{i,t}$, and $\theta^0_{n,t}$) are fixed in the original stochastic problem, which is solved to determine the operating-stage variables and the optimal objective-function value of the stochastic model, which we denote z^*_D. If we let z^*_S denote the optimal objective-function value obtained from solving the stochastic problem (without fixing the scheduling-stage variables using the deterministic model), then the VSS is given by:

$$\frac{z^*_D - z^*_S}{z^*_S}.$$

III. Examples

This section analyzes two simple examples, which illustrate the model detailed in Section II. The first is what we term a 'low-gas-price' example, in which both thermal and natural gas-fired generators are sufficiently flexible to serve the load. However, potential restrictions on natural gas use limit the extent to which the system can rely on natural gas-fired generators to serve load. The second, which we call a 'high-gas-price' example, requires the use of flexible but expensive natural gas-fired units to accommodate fast-ramping events that cannot be met by thermal units alone.

Both examples are based on the four-node electricity network shown in Fig. 1. The network includes two thermal units, located at nodes of their own, two natural gas-fired units, that are located at the same node and served by a single natural gas pipeline, and a single demand node. The corresponding transmission line data are provided in Table I, although there is no transmission congestion in this example. We study the commitment and dispatch of the system over a 12-hour planning horizon. We assume that the single pipeline serving the two natural gas-fired units can have binding hourly flow capacities. Fig. 2 shows the hourly pipeline capacities under the three scenarios that we model. Scenario 1 represents

tarjomehrooz.com 0902 795 28 76 ترجمه تخصصی توسط دکتری رشته مربوطه و برای کلیه زبان های خارجی + شبیه سازی مقالات با کلیه نرم افزار ها مثلب گمز و ...

an 'uncapacitated' scenario, in which the hourly pipeline capacities are not binding even if the two natural gas-fired units are operating at maximum load. The other two scenarios represent cases in which some contingency restricts pipeline use, especially in the middle of the planning horizon.

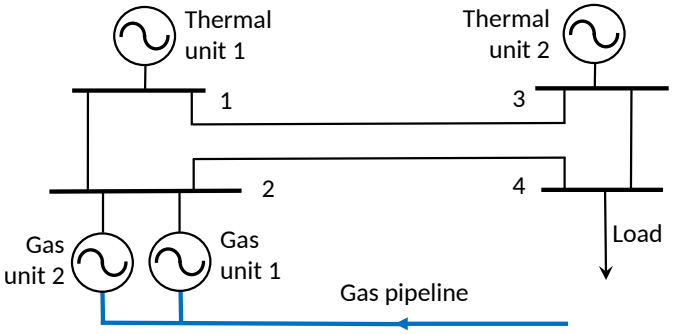

Fig. 1. Four-node power system and single natural gas pipeline used in the examples of Section III.

TABLE I
FOUR-NODE POWER SYSTEM TRANSMISSION DATA

From Node	To Node	B	$C^{\max}$
1	2	4.48	1200
1	3	5.05	1200
2	4	5.75	1200
3	4	5.67	1200

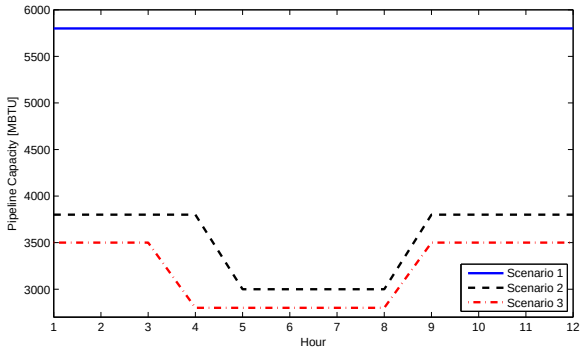

Fig. 2. Natural gas pipeline hourly capacity scenarios.

We now detail the other data and results of the two examples.

A. Low-Gas-Price Example

1) Data: Table II summarizes the cost and constraint data for the thermal and natural gas-fired units in the low-gas-price example. The natural gas price used in this case is \$4/MBTU. Fig. 3 shows the load data used. Due to their relatively low operating costs, the system operator prefers using the natural gas-fired generators to serve the system load. However, the possibility of binding natural gas-supply constraints in Scenarios 2 and 3 (*cf.* Fig. 2) may limit their use.

TABLE II
THERMAL AND NATURAL GAS-FIRED UNIT DATA FOR THE LOW-GAS-PRICE EXAMPLE

Unit	Marginal Cost	Start-Up Cost	RU, RD	$P^{\max}$	$P^{\min}$
Thermal					
1	75.0	800	100	600	30
2	80.5	900	100	600	20
Natural Gas					
1	55.0	560	250	600	25
2	50.0	420	250	600	25

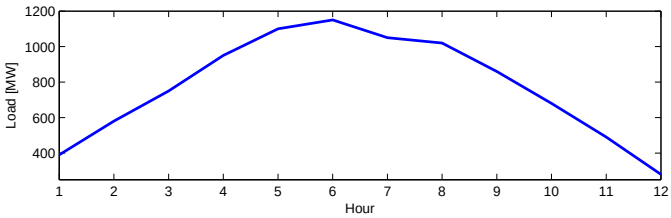

Fig. 3. Load data for the low-gas-price example.

2) Results: We examine system operations and market outcomes under two probability distributions for the pipeline-capacity scenarios. The first distribution assumes an 80% probability that the pipeline is uncapacitated, otherwise each of scenarios 2 and 3 are equally likely with 10% probabilities each. Thus, this first distribution has scenario-probability vector $\pi = (0.8, 0.1, 0.1)$. The second distribution assumes that the pipeline is uncapacitated with probability 1, or $\pi = (1.0, 0.0, 0.0)$.

The thermal units are not committed when the pipeline is uncapacitated with probability 1, *i.e.*, with the second probability distribution vector, $\pi = (1.0, 0.0, 0.0)$. When there is a nonzero probability that the pipeline will be capacitated, this results in committing the thermal units. In this latter case the two thermal units are committed between hours 3 and 10 and from hours 3 to 9, respectively. These thermal units are committed with the latter distribution because there is a nonzero probability that a binding pipeline-capacity constraint will prevent the natural gas-fired units from serving all of the loads in hours 3 through 10. Table III provides detailed unit commitment decisions.

TABLE III
OPTIMAL UNIT COMMITMENT DECISIONS FOR THE LOW-GAS-PRICE EXAMPLE

	Distribution 1 $\pi = (0.8, 0.1, 0.1)$				Distribution 2 $\pi = (1.0, 0, 0)$			
	Thermal		Natural Gas		Thermal		Natural Gas	
Hour	1	2	1	2	1	2	1	2
1	0	0	1	1	0	0	1	1
2	0	0	1	1	0	0	1	1
3	1	1	1	1	0	0	1	1
4	1	1	1	1	0	0	1	1
5	1	1	1	1	0	0	1	1
6	1	1	1	1	0	0	1	1
7	1	1	1	1	0	0	1	1
8	1	1	1	1	0	0	1	1
9	1	1	1	1	0	0	1	1
10	1	0	1	1	0	0	1	1
11	0	0	0	1	0	0	0	1
12	0	0	0	1	0	0	0	1

tarjomehrooz.com 0902 795 28 76 ترجمه تخصصی توسط دکتری رشته مربوطه و برای کلیه زبان های خارجی + شبیه سازی مقالات با کلیه نرم افزار ها متلب گمز و...

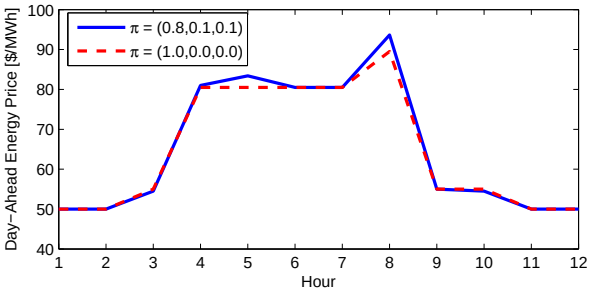

Fig. 4. Day-ahead prices at the demand node in the low-gas-price example.

Fig. 4 shows hourly day-ahead prices at the demand node under the two pipeline-capacity distributions. As expected, prices tend to be higher with the capacitated probability distribution. This is because the pipeline-capacity constraints result in greater use of higher-cost thermal units, which set the margin during hours when the pipeline could be binding. It is important to stress that the possibility of binding pipeline constraints impact day-ahead prices, regardless of whether those binding constraints are actually realized in real-time.

The VSS for this example, with probability distribution vector $\pi = (0.8, 0.1, 0.1)$, is 0.0638 (the VSS is, by definition, 0 with probability distribution vector $\pi = (1.0, 0.0, 0.0)$, because there is no uncertainty in this case). This means that when there is uncertainty regarding available natural gas, explicitly modeling this uncertainty in determining unit commitments reduces expected operating costs by 6.38%. Expected operation costs increase if the system is committed using expected pipeline capacities (in the deterministic model) because less thermal generation is committed (compared to the stochastic model). As a result, loads must be curtailed in some of the scenarios in which the natural gas pipeline is capacitated.

B. High-Gas-Price Example

1) Data: This example assumes the same physical power system structure shown in Fig. 1 and summarized in Table I and the same pipeline-capacity scenarios shown in Fig. 2. Table IV and Fig. 5 summarize the generator and load data, respectively, for this example. This example has higher natural gas prices of $12/MBTU, resulting in a cost reversal between the thermal and natural gas-fired units relative to the low-gas-price example. The load profile in this example has steeper ramps before and after the peak, which requires the use of the expensive natural gas-fired units.

TABLE IV
THERMAL AND NATURAL GAS-FIRED UNIT DATA FOR THE HIGH-GAS-PRICE EXAMPLE

Unit	Marginal Cost	Start-Up Cost	RU, RD	$P^{\max}$	$P^{\min}$
Thermal					
1	75.0	600	100	600	30
2	80.5	700	100	600	20
Natural Gas					
1	105.0	680	250	600	25
2	100.0	440	250	600	25

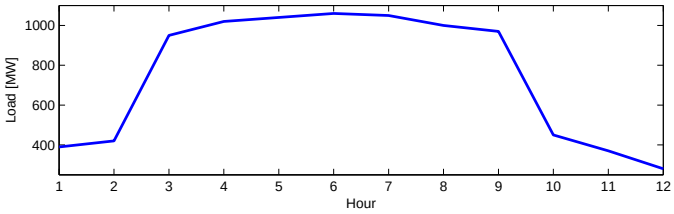

Fig. 5. Load data for the high-gas-price example.

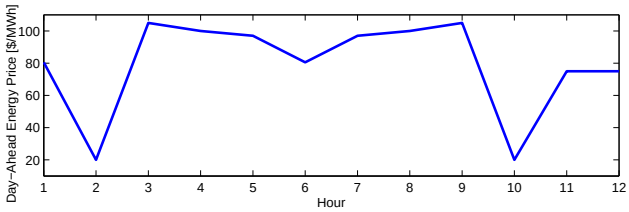

Fig. 6. Day-ahead prices at the demand node in the high-gas-price example.

2) Results: We examine system operations and market outcomes assuming that the natural gas pipeline is uncapacitated with probability 1, *i.e.*, with $\pi = (1.0, 0.0, 0.0)$. Because of the steep ramps in hours 3, 4, 8, and 9 and the limited ramping capabilities of the thermal units, the more expensive natural gas-fired units must be committed. Table V summarizes the optimal unit commitment decisions. Fig. 6 shows the resulting effect on day-ahead energy prices at the demand node. Prices are seen to rise exactly during the hours when binding ramping constraints require the use of expensive natural gas-fired units. Prices in hours 2 and 10 are lower than the marginal cost of the thermal units. This is because increasing demand in either of hours 2 or 10 allows greater use of thermal generation (in place of natural gas-fired generation) in hours 3 and 9. The prices reflect this value of shifting loads to hours 2 and 10. Sioshansi *et al.* provide a formal analysis of this pricing rule when ramping constraints are binding [20].

TABLE V
OPTIMAL UNIT COMMITMENT DECISIONS FOR THE HIGH-GAS-PRICE EXAMPLE

	Thermal		Natural Gas	
Hour	1	2	1	2
1	1	1	0	0
2	1	1	0	0
3	1	1	1	1
4	1	1	0	1
5	1	1	0	1
6	1	1	0	0
7	1	1	0	1
8	1	1	0	1
9	1	1	1	1
10	1	1	0	0
11	1	0	0	0
12	1	0	0	0

IV. CASE STUDY

In this section we further analyze the effects of the low- and high-gas-price examples examined in Section III, using case studies that are modeled around real-world power systems. More specifically, we examine a reduced eight-zone model of

tarjomehrooz.com 0902 795 28 76 ترجمه تخصصی توسط دکتری رشته مربوطه و برای کلیه زبان های خارجی + شبیه سازی مقالات با کلیه نرم افزار ها متلب گمز و ...

the ISO New England system [17] and a 240-node representation of the WECC, which includes the California ISO system [18]. Both cases assume a 24-hour optimization horizon in the unit commitment model.

A. Eight-Zone Test System

The eight-zone case study, which is modeled around the ISO New England system, is used to further study the effects of the low-gas-price case. The setting studied in Section III-A is reminiscent of recent events in the ISO New England system, in which the system is not able to rely on normally low-cost natural gas-fired units due to binding pipeline-capacity constraints [1].

1) Data: This case examines an eight-zone model of the ISO New England system [17].[1]. For sake of simplicity and to focus on the effect of natural gas-supply shortages, only thermal and natural gas-fired units are considered in our case study. The units in the system are aggregated into 37 units total—17 thermal and 20 natural gas-fired. Table VI summarizes the location, marginal generation cost, ramping limits (upward and downward ramping limits are assumed to be the same for each unit), and generating capacity of each unit. All of the units are assumed to have a minimum output level of 0 MW.

Loads are modeled using actual historical load data,[2] which are scaled based on the generation capacity modeled in this case study. Fig. 7 shows the load profile, which is aggregated over the eight zones in the network. Our case study uses the electric system topology reported by Krishnamurthy *et al.* [17]. We assume two natural gas pipelines. Natural gas-fired units 1–5 are supplied by one pipeline and units 6 and 20 are supplied by the other. We assume that there are 10 equally likely pipeline-capacity scenarios. These scenarios result in a variety of pipeline-capacity conditions. Some scenarios have binding pipeline capacities during the full 24-hour optimization horizon, others have binding pipeline capacity constraints during peak hours, and some have uncapacitated natural gas pipelines. The scenarios are selected to be realistic (*i.e.*, to mimic recent conditions under which the ISO New England system experiences binding pipeline constraints) and to obtain the desired price behavior. Needless to say, other scenario selections may result in different price behavior.

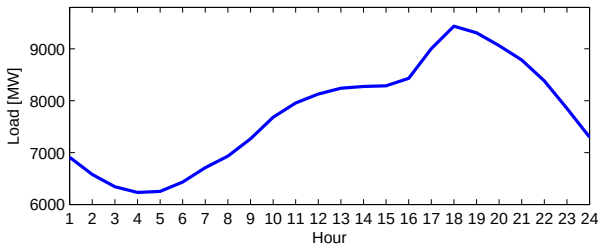

Fig. 7. Load data for the ISO New England-based eight-zone case study.

[1]https://bitbucket.org/kdheepak89/eightbustestbedrepo/src/
[2]http://iso-ne.com/isoexpress/web/reports/load-and-demand/

TABLE VI
UNIT LOCATION, COST, AND CONSTRAINT DATA FOR ISO NEW ENGLAND-BASED EIGHT-ZONE CASE STUDY

Unit	Zone	Marginal Cost	RU, RD	$P^{\max}$
Thermal				
1	ME	160.55	120.0	600.4
2	ME	233.00	120.0	431.0
3	ME	154.16	115.5	115.5
4	VT	185.00	120.0	620.2
5	NH	54.57	120.0	400.2
6	SEMA	153.16	120.0	558.7
7	SEMA	192.06	120.0	553.0
8	RI	192.00	120.0	435.0
9	CT	160.00	120.0	447.9
10	CT	233.42	120.0	407.4
11	CT	200.14	120.0	400.0
12	CT	192.06	120.0	236.0
13	CT	151.16	120.0	168.0
14	CT	152.16	120.0	130.5
15	CT	192.06	117.0	117.0
16	CT	54.00	81.0	81.0
17	CT	325.00	120.0	225.0
Natural Gas				
1	ME	51.13	400.0	693.8
2	ME	53.14	400.0	685.3
3	ME	51.00	400.0	490.4
4	ME	80.00	244.9	244.9
5	NH	51.13	400.0	508.0
6	WCMA	53.00	238.3	238.3
7	WCMA	123.00	141.0	141.0
8	SEMA	85.00	400.0	675.5
9	SEMA	86.00	244.8	244.8
10	SEMA	85.25	141.1	141.1
11	SEMA	85.50	104.9	104.9
12	RI	55.72	400.0	515.5
13	RI	55.72	270.9	270.9
14	RI	85.00	264.9	264.9
15	RI	50.23	248.7	248.7
16	RI	85.50	238.6	238.6
17	RI	84.50	149.0	149.0
18	RI	85.00	149.0	149.0
19	CT	78.00	400.0	447.9
20	CT	85.03	43.9	43.9

2) Results: Fig. 8 shows load-weighted day-ahead LMPs. As expected, prices increase during peak-load hours and decrease in off-peak hours. The LMPs in hour 9 are dramatically high because the upward ramping constraints for thermal units 4, 10, and 12 are binding in scenario 10. Scenario 10 is the one in which natural gas availability is highly limited. The proposed model commits natural gas-fired units during all 24 hours of the optimization horizon. Lower-cost natural gas-fired units are prioritized in the commitment and dispatch over higher-cost units. Although the natural gas pipelines are not capacitated in all scenarios, low-cost natural gas-fired unit are not fully loaded in the scheduling stage. Rather, the dispatch of each natural gas-fired unit is adjusted in the operating stage depending on how much pipeline capacity is available in the recourse stage. The model limits the commitment and dispatch of higher-cost thermal units, which is consistent with the cost-minimization objective.

On the other hand, reducing the capacities of the electricity transmission lines that directly connect zones ME and NH results in transmission congestion. Fig. 9 shows load-weighted average (across the entire system footprint) day-ahead LMPs as well as day-ahead LMPs for the ME zone and the load-weight average LMPs of the other zones. The nodal price

tarjomehrooz.com 0902 795 28 76 ترجمه تخصصی توسط دکتری رشته مربوطه و برای کلیه زبان های خارجی + شبیه سازی مقالات با کلیه نرم افزار ها مثلب گمز و...

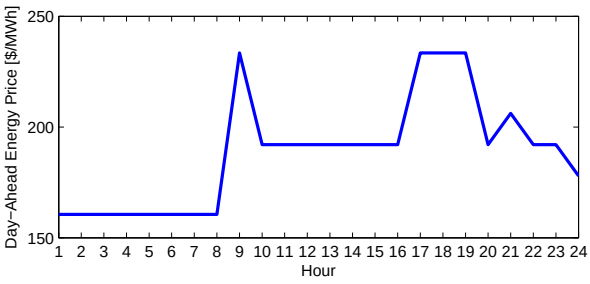

Fig. 8. Load-weighted day-ahead LMPs in the ISO New England-based eight-zone case study.

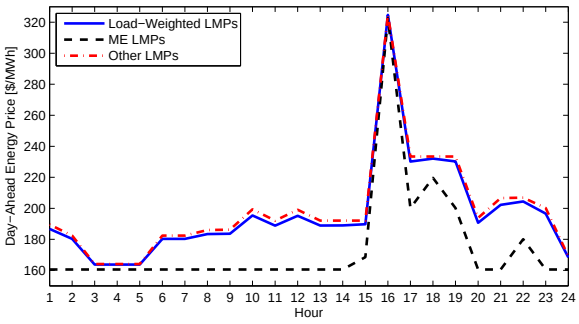

Fig. 9. Load-weighted day-ahead LMPs for the entire system footprint, ME zone, and other zones in the ISO New England-based eight-zone case study with restricted transmission capacity.

differences are caused by transmission-line congestion. The commitment status of the thermal and gas-fired units are similar between the congested and uncongested cases, showing that the commitment decisions are fundamentally driven by natural gas-pipeline capacities. The high prices in hour 16 are caused by binding upward ramping limit for all of the thermal units that are on-line as well as limited natural gas availability in some scenarios. Additional thermal unit would be started-up if the load in hour 16 is further increased.

The VSS for the cases with and without transmission congestion are 0.0724 and 0.074, respectively. As with the low-gas-price example examined in Section III-A, if the system is committed using a deterministic model with expected pipeline capacities, fewer thermal units are committed as compared to those committed by the stochastic model. As a result, there is non-zero energy curtailment in some of the scenarios in which the natural gas pipelines are capacitated.

The model is programmed using GAMS version 24.4.6 and solved using CPLEX version 12.6.2.0 on a computer with an Intel Core i7 2.6 GHz processor with 8 GB of RAM. The computation time of each of the eight-zone cases is approximately 15 minutes.

B. 240-Node Test System

The 240-node case study, which is modeled around the WECC system, is used to further study the effects of the high-gas-price case. The assumptions underlying the analysis in Section III-B are reminiscent of what is expected to occur in the California ISO system in the near future. As the penetrations of solar photovoltaic and wind generators increase, high ramps in the net load (*i.e.*, load less renewable production) profile are expected in the mornings and evenings. These ramps are anticipated to be met using relatively high-cost natural gas-fired generators [15], [16].

1) Data: This case study is based on a 240-node reduced model of the WECC system [18] and analyzes the effect of high natural gas prices. To reduce computational complexity, the system is modeled as consisting of 31 units—16 thermal and 15 natural gas-fired. The loads are modeled as being at 25 of the nodes. Unit, transmission line, and load data are based on the reduced WECC model provided by Price and Goodin [18]. Fig. 10 shows the aggregated (over the 25 load nodes) load profile, which has steep ramps in the morning and afternoon.

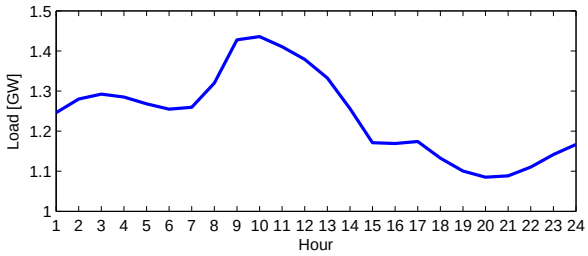

Fig. 10. Load data for the WECC-based 240-node case study.

Table VII shows marginal cost, ramping limit, capacity, and minimum generation level data for the thermal and natural gas-fired units. The system is assumed to have two natural gas pipelines. The first pipeline is shared by natural gas-fired units 1–7 while the other serves natural gas-fired units 8–15. Due to the relatively low demand of natural gas in this high-gas price case study, we only consider one scenario in which the natural gas pipelines are uncapacitated with probability 1. The case study assumes a natural gas price of $11/MBTU, based on historical natural gas prices in California.[3]

2) Results: Because of their relatively high cost, only natural gas-fired unit 11, the cheapest among all of the natural gas-fired units, is committed in hours 9, 13, and 14. This unit is committed solely because of the steep ramps and the need for its greater ramping capability (compared to the thermal units). Fig. 11 shows load-weighted average day-ahead LMPs, which are computed once binary variables are fixed to their optimal values. There is no transmission line congestion in this case, so all the LMPs at each of the 240 nodes in each same hour are the same. As in the high-gas-price example examined in Section III-B, day-ahead prices spike when natural gas-fired units must be committed to accommodate steep ramps. Moreover, we find that day-ahead prices in hours 8 and 15 are much lower than the marginal cost of any unit (indeed, they are negative). This is because of the same phenomenon that higher loads in these hours allows more lower-cost thermal generation to substitute high-cost natural gas-fired generation in hours 9 and 14. High LMPs in hours 10 and 11 due to binding ramping limits of thermal units, and higher load in these hours require the use of high-cost natural gas-fired generation.

[3]https://www.eia.gov/dnav/ng/hist/n3045ca3m.htm

tarjomehrooz.com 0902 795 28 76 ترجمه تخصصی توسط دکتری رشته مربوطه و برای کلیه زبان های خارجی + شبیه سازی مقالات با کلیه نرم افزار ها مثلب گمز و ...

TABLE VII
UNIT LOCATION, COST, AND CONSTRAINT DATA FOR WECC-BASED 240-NODE CASE STUDY

Unit	Node	Marginal Cost	RU, RD	$P^{\max}$	$P^{\min}$
Thermal					
1	180	80	50	1100	25
2	202	83	50	900	25
3	230	80	50	800	25
4	160	79	50	1100	25
5	164	79	50	1000	25
6	167	84	50	800	25
7	172	85	50	800	25
8	188	85	50	800	25
9	192	77	50	900	25
10	208	79	50	800	25
11	215	82	50	800	25
12	221	80	50	800	25
13	223	76	50	1200	25
14	239	80	50	1000	25
15	240	79	50	800	25
16	237	82	50	900	25
Natural Gas					
1	191	170	200	1000	20
2	201	145	400	900	20
3	204	165	400	1200	20
4	210	180	400	1200	20
5	214	175	400	1200	20
6	224	160	400	1600	20
7	238	165	400	1200	20
8	159	185	200	1200	20
9	187	165	200	800	20
10	218	173	200	800	20
11	220	144	400	500	20
12	229	173	400	950	20
13	175	166	400	1400	20
14	225	173	400	900	20
15	233	167	200	1000	20

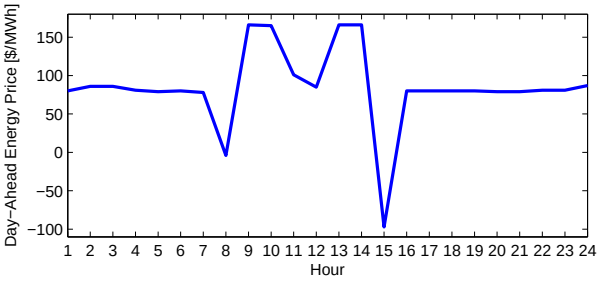

Fig. 11. Load-weighted day-ahead LMPs in the WECC-based 240-node case study.

As in the case examined in Section IV-A, reducing the capacity of the transmission lines directly connecting node 77 to 55 and node 77 to 145 causes congestion to occur in hour 10. This results in LMP differences across the nodes in hour 10. Fig. 12 shows load-weighted LMPs and LMPs at two nodes—55 and 77—that have large price differences in hour 10. Node 77 is connected to a low-cost thermal unit through an uncongested transmission line. Thus, increased demand in this node can be served by this low-cost thermal unit. However, additional demand in node 55 can only be served by high-cost natural gas-fired units, due to binding transmission and ramping constraints. This explains the significant LMPs differences between these two nodes. The congested case also sees some differences in the units committed compared to the uncongested case, again due to locational constraints that require the use of natural gas-fired units to serve the fast-ramping event.

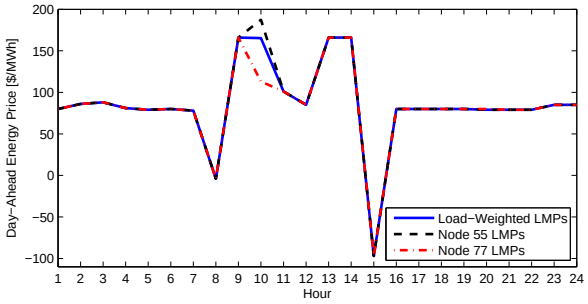

Fig. 12. Load-weighted day-ahead LMPs for the entire system footprint and for nodes 55 and 77 in the WECC-based 240-node case study with restricted transmission capacity.

The case study is implemented in the same environment that the eight-zone case study is, and requires about three minutes of computation time.

V. CONCLUSIONS

This paper proposes a two-stage stochastic unit commitment model that integrates natural gas-supply conditions into power system operations. Our modeling framework assumes that unit commitment decisions are made day-ahead, in the face of natural gas-capacity-constraint uncertainties. The second stage of our model allows the dispatch of the committed units to respond to real-time natural gas availability.

We use this model to study the effects on power system operations of two types of natural gas-supply conditions. The first has low natural gas prices, but potential natural gas-supply bottlenecks. These possible natural gas-supply constraints necessitate the use of higher-cost thermal units and have an effect on day-ahead prices. It is important to stress that these effects occur regardless of whether any natural gas pipeline is actually capacitated in real-time. The second assumes relatively high natural gas prices. The system must use expensive natural gas-fired generation, due to the operating flexibility of those units (relative to thermal units) to handle fast-ramping events. We demonstrate the effects of these fast-ramping events on day-ahead LMPs. We do not study the impacts of uplifts, which are necessitated by the non-convex nature of unit commitments to ensure that the commitment and dispatch is economically nonconfiscatory. While such uplifts will have some impacts on market settlement, they should not alter the general conclusions derived [21].

The two types of natural gas-supply conditions that we modeled are inspired by conditions facing the ISO New England and California ISO systems. It is important to note, however, that these types of fuel-supply conditions may increasingly become an issue in other power systems. Models, such as the one that we propose here, could be used to help system operators, generators, and utilities mitigate the effects of such conditions. Indeed, a key contribution of the model proposed here is providing a tool to 'quantify' the impact of natural gas-supply uncertainty and natural gas prices on LMPs and the scale and extent of such impacts.

tarjomehrooz.com 0902 795 28 76 ترجمه تخصصی توسط دکتری رشته مربوطه و برای کلیه زبان های خارجی + شبیه سازی مقالات با کلیه نرم افزار ها مثلب گمز و ...

Comprehensive modeling of the natural gas pipeline system will make the proposed model more realistic, but will not change the conclusions derived. Enhancing the modeling of the natural gas-pipeline system is an area for further research. It should also be noted that any technique aimed at improving computational efficiency or achieving tractability in large-scale systems (*e.g.*, decomposition or scenario-reduction techniques) can be applied to the proposed model.

REFERENCES

[1] *Phase 2 Report: Interregional Transmission Development and Analysis for Three Stakeholder Selected Scenarios And Gas-Electric System Interface Study*, Eastern Interconnection Planning Collaborative, 2 July 2015.

[2] A. Alabdulwahab, A. Abusorrah, X. Zhang, and M. Shahidehpour, "Stochastic Security-Constrained Scheduling of Coordinated Electricity and Natural Gas Infrastructures," *IEEE Systems Journal*, 2016, in press.

[3] J. Munoz, N. Jimenez-Redondo, J. Perez-Ruiz, and J. Barquin, "Natural Gas Network Modeling for Power Systems Reliability Studies," in *2003 IEEE Bologna Power Tech Conference Proceedings*. Bologna, Italy: Institute of Electrical and Electronics Engineers, 23-26 June 2003.

[4] A. M. Quelhas, E. Gil, and J. D. McCalley, "Nodal prices in an integrated energy system," *International Journal of Critical Infrastructures*, vol. 2, pp. 50–69, 2006.

[5] M. Geidl and G. Andersson, "Optimal Power Flow of Multiple Energy Carriers," *IEEE Transactions on Power Systems*, vol. 22, pp. 145–155, February 2007.

[6] C. Liu, M. Shahidehpour, Y. Fu, and Z. Li, "Security-Constrained Unit Commitment With Natural Gas Transmission Constraints," *IEEE Transactions on Power Systems*, vol. 24, pp. 1523–1536, August 2009.

[7] T. Li, M. Eremia, and M. Shahidehpour, "Interdependency of Natural Gas Network and Power System Security," *IEEE Transactions on Power Systems*, vol. 23, pp. 1817–1824, November 2008.

[8] M. Qadrdan, J. Wu, N. Jenkins, and J. Ekanayake, "Operating Strategies for a GB Integrated Gas and Electricity Network Considering the Uncertainty in Wind Power Forecasts," *IEEE Transactions on Sustainable Energy*, vol. 5, pp. 128–138, January 2014.

[9] A. Alabdulwahab, A. Abusorrah, X. Zhang, and M. Shahidehpour, "Coordination of Interdependent Natural Gas and Electricity Infrastructures for Firming the Variability of Wind Energy in Stochastic Day-Ahead Scheduling," *IEEE Transactions on Sustainable Energy*, vol. 6, pp. 606–615, April 2015.

[10] C. Liu, C. Lee, and M. Shahidehpour, "Look Ahead Robust Scheduling of Wind-Thermal System With Considering Natural Gas Congestion," *IEEE Transactions on Power Systems*, vol. 30, pp. 544–545, January 2015.

[11] J. Ostrowski, M. F. Anjos, and A. Vannelli, "Tight Mixed Integer Linear Programming Formulations for the Unit Commitment Problem," *IEEE Transactions on Power Systems*, vol. 27, pp. 39–46, February 2012.

[12] J. M. Morales, A. J. Conejo, H. Madsen, P. Pinson, and M. Zugno, *Integrating Renewables in Electricity Markets: Operational Problems*, ser. International Series in Operations Research & Management Science. New York, New York: Springer Science+Business Media, LLC, 2014, vol. 205.

[13] M. Vrakopoulou, K. Margellos, J. Lygeros, and G. Andersson, "A Probabilistic Framework for Reserve Scheduling and $N-1$ Security Assessment of Systems With High Wind Power Penetration," *IEEE Transactions on Power Systems*, vol. 28, pp. 3885–3896, November 2013.

[14] D. Bienstock, M. Chertkov, and S. Harnett, "Chance-Constrained Optimal Power Flow: Risk-Aware Network Control under Uncertainty," *SIAM Review*, vol. 56, pp. 461–495, 2014.

[15] J. Bushnell, S. M. Harvey, S. Stoft, and B. F. Hobbs, "Final Opinion on Payment for Provision of Flexible Ramping," Tech. Rep., 16 August 2011.

[16] P. Denholm, M. O'Connell, G. Brinkman, and J. Jorgenson, "Overgeneration from Solar Energy in California: A Field Guide to the Duck Chart," National Renewable Energy Laboratory, Tech. Rep. NREL/TP-6A20-65023, November 2015.

[17] D. Krishnamurthy, W. Li, and L. Tesfatsion, "An 8-Zone Test System Based on ISO New England Data: Development and Application," *IEEE Transactions on Power Systems*, vol. 31, pp. 234–246, January 2016.

[18] J. E. Price and J. Goodin, "Reduced network modeling of WECC as a market design prototype," in *2011 IEEE Power and Energy Society General Meeting*. San Diego, California: Institute of Electrical and Electronics Engineers, 24-29 July 2011.

[19] A. J. Conejo, M. Carrión, and J. M. Morales, *Decision Making Under Uncertainty in Electricity Markets*, ser. International Series in Operations Research & Management Science. New York, New York: Springer Science+Business Media, LLC, 2010, vol. 153.

[20] R. Sioshansi, S. Oren, and R. O'Neill, "Three-Part Auctions versus Self-Commitment in Day-ahead Electricity Markets," *Utilities Policy*, vol. 18, pp. 165–173, December 2010.

[21] F. Abbaspourtorbati, A. J. Conejo, J. Wang, and R. Cherkaoui, "Pricing Electricity through a Stochastic Non-Convex Market-Clearing Model ," *IEEE Transactions on Power Systems*, 2016, in press.

Bining Zhao received the B.S. degree in Electrical Engineering and Automation from North China Electric Power University, Baoding, China, in 2014. She is currently working toward her Ph.D. degree in the Electrical and Computer Engineering Department at The Ohio State University, Columbus, OH.

Antonio J. Conejo (F'04) received the M.S. degree from the Massachusetts Institute of Technology, Cambridge, MA, in 1987, and the Ph.D. degree from the Royal Institute of Technology, Stockholm, Sweden, in 1990.

He is currently a full professor in the Integrated System Engineering and the Electrical and Computer Engineering Departments, The Ohio State University, Columbus, OH. His research interests include control, operations, planning, economics and regulation of electric energy systems, as well as statistics and optimization theory and its applications.

Ramteen Sioshansi (M'11–SM'12) holds the B.A. degree in economics and applied mathematics and the M.S. and Ph.D. degrees in industrial engineering and operations research from the University of California, Berkeley, and an M.Sc. in econometrics and mathematical economics from The London School of Economics and Political Science.

He is an associate professor in the Integrated Systems Engineering Department at The Ohio State University, Columbus, OH. His research focuses on renewable and sustainable energy system analysis and the design of restructured competitive electricity markets.